Nanoscale
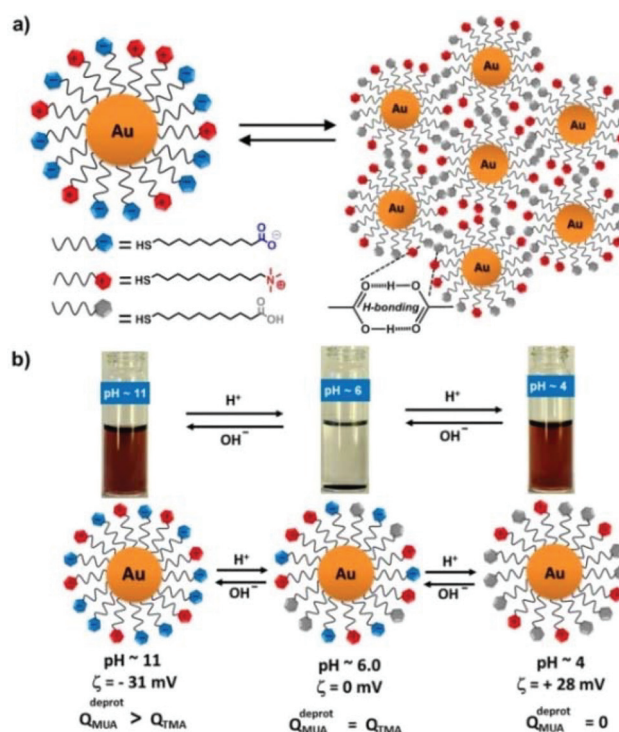
Self-assembly of like-charged nanoparticles into microscopic crystals†

Pramod P. Pillai,[a,b] Bartlomiej Kowalczyk*[a,c] and Bartosz A. Grzybowski*[d]

Like-charged nanoparticles, NPs, can assemble in water into large, faceted crystals, each made of several million particles. These NPs are functionalized with mixed monolayers comprising ligands terminating in carboxylic acid group ligands as well as positively charged quaternary ammonium ligands. The latter groups give rise to electrostatic interparticle repulsions which partly offset the hydrogen bonding between the carboxylic acids. It is the balance between these two interactions that ultimately enables self-assembly. Depending on the pH, the particles can crystallize, form aggregates, remain unaggregated or even – in mixtures of two particle types – can "choose" whether to crystallize with like-charged or oppositely charged particles.

Self-assembly of nanoparticles into three-dimensional (3D) crystals is motivated by the potential uses of these structures in bio-sensing,[1] optoelectronics,[2] chemical amplifiers,[3] or catalysis.[4] The methods of obtaining such structures employ covalent or non-covalent molecular interactions,[5,6] dipole–dipole interactions,[7] or electrostatic forces,[3,8–13] many exhibiting effects peculiar to the nanoscale.[14–19] While in numerous cases, the formation of 3D NP crystals was achieved using only one type of particle, these systems were typically based on NPs suspended in non-polar solvents and interacting *via* van der Waals forces.[20] On the other hand, crystallization in aqueous solutions has generally required the use of binary NP mixtures – *e.g.*, mixtures of particles functionalized with oppositely charged ligands[3,5,8,12,15] or with complementary DNA strands.[9,21–24] Here, we attempted to assemble NP crystals in

aqueous solutions from only one type of particle. The distinctive feature of our method is that rather than having different/complimentary chemical functionalities on different NPs, our particles combine two types of functionalities on each NP (Fig. 1a). One of these functionalities (carboxylic acids) is capable of hydrogen bonding whereas the other (quaternary ammonium salts) gives rise to electrostatic repulsions between the NPs. Perhaps counterintuitively, micron-sized NP crystals

[a]*Department of Chemistry and Department of Chemical Engineering, Northwestern University, 2145 Sheridan Road, Evanston, Illinois, USA*
[b]*Department of Chemistry, Indian Institute of Science Education and Research (IISER) Pune, Dr. Homi Bhabha Road, Pashan, Pune, 411008, India*
[c]*3M Purification Inc., 400 Research Parkway, Meriden, CT 064503, USA. E-mail: bkowalczyk@mmm.com*
[d]*IBS Center for Soft and Living Matter and the Department of Chemistry, Ulsan National Institute of Science and Technology (UNIST), Ulsan, South Korea. E-mail: grzybor72@unist.ac.kr*

†Electronic supplementary information (ESI) available: Further experimental details, images of crystals as well as NMR and EDX spectra. See DOI: 10.1039/c5nr06983a

Fig. 1 (a) Scheme of nanoparticles decorated with mixed SAMs comprising ligands illustrated in the legend. Crystals form when carboxylic acid groups are protonated and capable of hydrogen bonding. (b) Owing to the presence of both acidic and basic groups, the NPs are stable in water both at low and high pH values and precipitate only at the pH at which the net charge on the NPs is zero (see ref. 26).

form when the NPs are all like-charged. Under these conditions, however, interparticle electrostatic repulsions serve to partly offset and "balance" the hydrogen bonding (attractive) interactions that would – by themselves – have resulted in aggregation/flocculation rather than crystallization. Interestingly, as the pH and the balance between H-bonding and electrostatic interactions change, the mixed charge (MC) NPs can "choose" whether and with which other types of NPs present in solution to co-crystallize. Overall, our approach illustrates that by appropriately designing mixed-ligand shells on nanoscale objects it is possible to modify interparticle potentials and flexibly guide nanoscale self-assembly involving several types of interactions.

We used gold nanoparticles (AuNPs) synthesized according to a previously published procedure.[25] These NPs were initially stabilized with dodecylamine (DDA) ligands and were prepared in five batches characterized by different core diameters, 4.2 ± 0.5 nm, 5.5 ± 0.5 nm, 8.0 ± 0.5 nm, 9.5 ± 0.8 nm and 11.5 ± 0.5 nm (average sizes and size distributions were determined by TEM analysis of ~200 nanoparticles for each size). Next, the NPs were functionalized via a ligand exchange reaction with mixed self-assembled monolayers (mSAMs)[26] comprising neutral 11-mercaptoundecanoic acid (MUA) and positively charged N,N,N-trimethyl(11-mercaptoundecyl)ammonium chloride (TMA). This was done by soaking the DDA/AuNPs in a 2 : 1 mol : mol mixture of MUA and TMA thiols ($\alpha_{soln} = C_{soln}^{MUA}/C_{soln}^{TMA} = 2$) in toluene/dichloromethane (20 mL/10 mL) for 15 h. The concentration of AuNPs (0.15 mM in terms of Au atoms) and the total concentration of thiols (0.15 mM) were kept constant, and the thiols were in ~40 fold excess with respect to the number of adsorption sites on the NPs. After ligand exchange, the unbound thiols were removed by several cycles of precipitation using dichloromethane followed by washing with copious amounts of acetone. The purified particles were then dissolved in water and the pH of all the solutions was adjusted to either pH = 4 (by addition of 0.2 M HCl) or pH = 11 (using 0.2 M tetramethylammonium hydroxide). As illustrated in Fig. 1b, the NPs were stable in water at both of these pH values. The composition of the two ligands in the mSAMs on the NP surfaces was determined by dissolving NP cores using molecular I_2 followed by ^1H NMR analysis (for details, see ESI†); it was found that the ratio of surface concentrations of MUA to TMA thiols was $\alpha_{surf} = C_{surf}^{MUA}/C_{surf}^{TMA} = 1.6$. NPs from all batches were also characterized by TEM, UV-Vis, DLS and zeta potential measurements.

For each crystallization, a solution of AuNPs (2–3 µmol in terms of gold atoms; prepared by diluting 150 µL of 15 mM stock with DI water to 2 mL) was diluted by adding half of the sample's volume (i.e., 1 mL) of dimethyl sulfoxide (DMSO). The solution was heated to 65 °C to slowly evaporate water and initialize the crystallization process. After ~36 h, the supernatant solution became colorless and a black powder settled at the bottom of the vial. The remaining DMSO was decanted carefully and the powder was washed several times with anhydrous acetonitrile to remove excess salts. SEM, TEM and Small Angle X-ray Diffraction Spectroscopy (SAXS) were used to determine whether the powder contained NP crystals (cf. ESI† for further experimental details).

The main result of this work is that NP crystals could form even when the particles were all positively charged. Specifically, at pH = 4, 4.2 nm, 5.5 nm and 8.0 nm NPs all formed regularly faceted crystals, each composed of several million NPs and with dimensions up to 3 µm in each direction (Fig. 2a and Fig. 3). Under these conditions, all carboxylic acids on NP surfaces were protonated[27] and the NPs had net positive charges as evidenced by the values of the zeta potential being greater than zero (typically, tens of mV; see Fig. 2a). The crystals were examined by small angle X-ray diffraction spectroscopy (SAXS) exhibiting four distinct peaks located at scattering vectors, q = 0.097 A^{-1}, 0.108 A^{-1}, 0.1728 A^{-1}, and 0.2021 A^{-1} for 5.5 NPs (Fig. 3d). This diffraction pattern characterizes the sphalerite structure[8] with lattice constant a = 19.2 nm and with peak positions corresponding to the Bragg reflections on planes specified by Miller indices (111), (200), (220), and (311), respectively. In contrast, larger (9.5 nm and 11.5 nm) NPs formed disordered assemblies such as those illustrated in Fig. 2c and d.
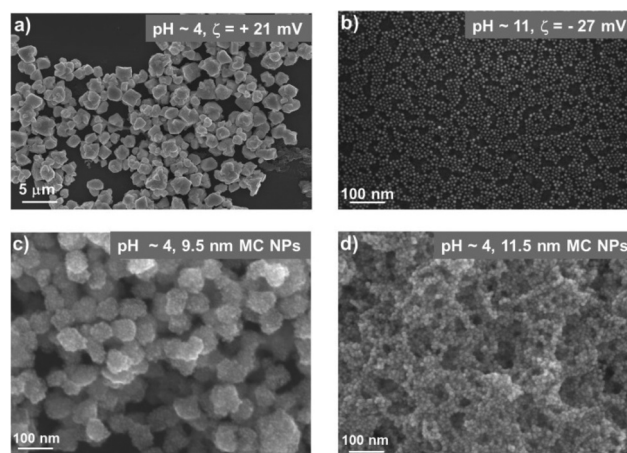

Fig. 2 Four major types of structures observed for different particle sizes and different pH values: (a) smaller NPs (up to ca. 8 nm) form regularly faceted crystals at pH = 4; (b) unaggregated NPs are observed for all particle sizes at pH = 11; (c, d) non-crystalline aggregates are obtained from larger NPs at pH = 4.

Finally, at high pH – when the carboxylic acids were fully deprotonated – the NPs were all negatively charged, had negative zeta potentials (Fig. 2b) and remained stable in solution rather than form crystals or disordered aggregates.

These observations can be rationalized based on the balance between attractive and repulsive interactions acting in the system (Fig. 4). The former include vdW and hydrogen bonding, while the latter are electrostatic forces. As discussed in detail in our previous studies,[14,27b] the energies of vdW interactions at small interparticle separations for ~6 nm AuNPs covered with 1.5 nm-thick SAMs in water are up to ~10kTs whereas the hydrogen bonding between such spherical particles contributes few additional kTs. The electrostatic
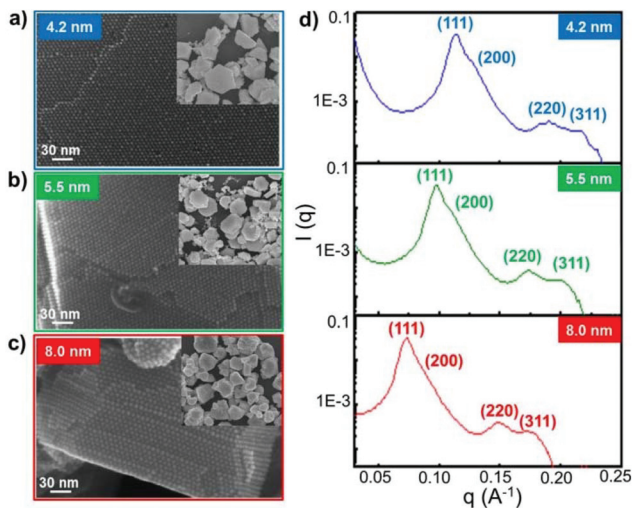
Fig. 3 Characterization of NP crystals. SEM images of 3D crystals resulting from self- assembly of (a) 4.2 nm, (b) 5.5 nm and (c) 8.0 nm AuNPs ($\alpha_{surf} = C_{surf}^{MUA}/C_{surf}^{TMA} = 1.6$) at pH ~ 4. Individual NPs are clearly visible at the crystals' surfaces. Corresponding large area SEM images are shown in the insets while (d) gives the small angle powder XRD spectra of the crystals. These spectra are congruent with the sphalerite crystal structure.

repulsions for such charged particles are *ca.* 10–20kTs strong. It follows that at low pH, the superposition of attractive and repulsive potentials gives rise to a "shallow" net potential (featuring a small energetic barrier; see for example ref. 27b). Effectively, the NPs are weakly attractive on the thermal, kT, scale and their self-assembly process is partly reversible allowing for the formation of ordered assemblies rather than the rapid aggregation that would be expected for strong particle attractions.[8] Such an aggregation is observed for larger particles because the vdW forces scale with particle size. At high pH values there is no hydrogen bonding between the fully deprotonated carboxylates and the electrostatic repulsions dominate.
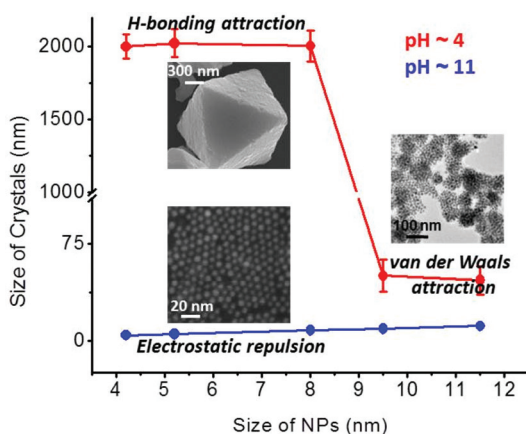

Fig. 4 Graph plotting the average sizes of the forming structures as a function of NP size for low (red line) and high (blue line) pH.

Few further remarks are in order. One question that arises is whether the mixed SAMs are indeed necessary to observe crystallization – in particular, one might imagine NPs covered with only COOH terminated thiols for which, at some intermediate pH, enough carboxylic acids would be deprotonated to give rise to electrostatic interparticle repulsions that balance out the sum of vdW and (remaining) hydrogen bonding attractions. In such a system, however, water solubility becomes a problem as the particles precipitate at lower pH values – there are potentially ways around this complication (*e.g.*, adjusting the dielectric constant of the solvent) but formation of crystals remains problematic as we have indeed experienced in many unsuccessful experiments with such particles. In contrast, as illustrated in Fig. 1b, the mixed-SAM NPs are readily soluble at both low and high pH values and at either negative or positive net particle charges. The only regime where these NPs precipitate is when the negative and positive charges are compensated and the net charge is zero.

The second question to address is the composition of the mSAMs – here, we used $\alpha_{surf} = C_{surf}^{MUA}/C_{surf}^{TMA} = 1.6$ but other ratios can be prepared, as described in detail in ref. 26a. At lower ratios, when there are more TMAs than MUAs on the particles' surfaces, the NPs do not crystallize. On the other hand, at ratios higher than 1.6, the hydrogen bonding at low pH dominates electrostatic repulsions and rapid precipitation rather than controlled NP crystallization ensues. This is illustrated in ESI Fig. S3† where for $\alpha_{surf} = C_{surf}^{MUA}/C_{surf}^{TMA} = 2.5$ the NPs form some disordered/non-crystalline aggregates whereas for $\alpha_{surf} = C_{surf}^{MUA}/C_{surf}^{TMA} = 7.7$, only a completely amorphous precipitate is observed. It follows that precipitation requires the "right" balance between electrostatic repulsions and vdW/ H-bonding attractions and there must be enough TMA groups on the surface to offset the hydrogen bonding.

The dependence of net charge on our NPs on the pH opens additional possibilities for controlling not only the self-assembly of such particles but also co-assembly with other charged species present. This is illustrated by experiments in which our TMA/MUA AuNPs were mixed with like-sized, TMA-covered Ag NPs (positively charged at all pH values). The use of different metal cores allowed us to quantify the elemental composition of the crystals that formed by Energy Dispersive X-ray (EDX) spectroscopy. At pH ~ 4, the MUA/TMA AuNPs had net positive charges (*cf.* Fig. 2a) and were capable of interacting with each other through hydrogen bonds. Under these conditions, the MUA/TMA AuNPs assembled predominantly between themselves rather than with the like-charged but non-hydrogen-bonding Ag TMA particles. Consequently, the crystals that formed (Fig. 5a) comprised ~85% of Au, with only ~12% of Ag (rest is S, Cl, C *etc.*; see Fig. S4† for elemental mapping). The presence of this small percentage of Ag NPs could be attributed to their physisorption onto the crystals precipitating from DMSO since TMA NPs are poorly soluble in this solvent. In contrast, at pH ~ 11, the MUA/TMA particles had negative charges, and were not able to assemble with each other, but readily co-crystallized with the positively charged TMA NPs to give crystals that contained roughly equal
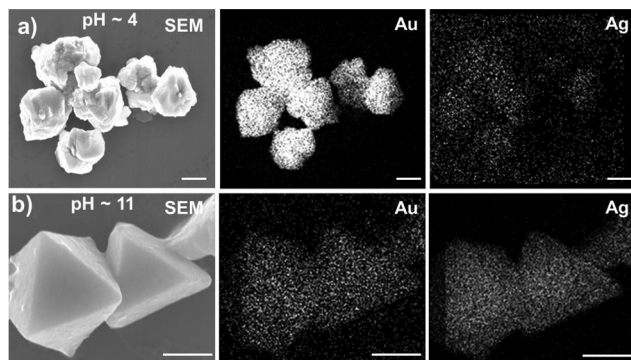
Fig. 5 Characterization of crystals formed from mixtures of MUA/TMA AuNPs and TMA AgNPs at (a) pH ~ 4 and (b) pH ~ 11, respectively. EDXS mapping confirms the presence of large quantities of Ag in crystals formed at pH ~ 11. Scale bar for (a) is 200 nm and for (b) is 1 μm.

proportions of each type of NPs (Fig. 5b and Fig. S5† for elemental mapping).

This last example illustrates the flexibility of mixed-charge NPs in the design of nanomaterials – the major virtue of these particles is that because they remain water-soluble at both low and high pH values, their charges and propensity to interact by hydrogen bonds can be tuned by adjusting the pH. An interesting avenue for future research, one that would build on the results from Fig. 5 of the current paper, would be to perform sequential self-assembly from mixtures of mixed-charged particles and other charged objects – for instance, by first assembling all-AuNP crystals (held tightly by vdW interactions once formed, see ref. 27b) at low pH and then depositing onto them – from the same solution – Au/Ag shells at high pH. This and similar strategies could underlie a new family of one-batch syntheses leading to nano-assemblies of complex internal structures.

Acknowledgements

Notes and references

1 M. Zayats, A. B. Kharitonov, S. P. Pogorelova, O. Lioubashevski, E. Katz and I. Willner, *J. Am. Chem. Soc.*, 2003, **125**, 16006.

2 S. A. Maier, P. G. Kik, H. A. Atwater, S. Meltzer, E. Harel, B. E. Koel and A. A. G. Requicha, *Nat. Mater.*, 2003, **2**, 229.

3 B. Kowalczyk, D. A. Walker, S. Soh and B. A. Grzybowski, *Angew. Chem., Int. Ed.*, 2010, **49**, 5737.

4 J. Grunes, J. Zhu, E. A. Anderson and G. A. Somorjai, *J. Phys. Chem. B*, 2002, **106**, 11463.

5 C. J. Kiely, J. Fink, M. Brust, D. Bethell and D. J. Schiffrin, *Nature*, 1998, **396**, 444.

6 Y. Zhao, K. Thorkelsson, A. J. Mastroianni, T. Schilling, J. M. Luther, B. J. Rancatore, K. Matsunaga, H. Jinnai, Y. Wu, D. Poulsen, J. M. J. Fréchet, P. Alivisatos and T. Xu, *Nat. Mater.*, 2009, **8**, 979.

7 D. A. Walker, K. P. Browne, B. Kowalczyk and B. A. Grzybowski, *Angew. Chem., Int. Ed.*, 2010, **49**, 6760.

8 A. M. Kalsin, M. Fialkowski, M. Paszewski, S. K. Smoukov, K. J. M. Bishop and B. A. Grzybowski, *Science*, 2006, **312**, 420.

9 R. J. Macfarlane, B. Lee, M. R. Jones, N. Harris, G. C. Schatz and C. A. Mirkin, *Science*, 2011, **334**, 204.

10 E. V. Shevchenko, D. V. Talapin, N. A. Kotov, S. O'Brien and C. B. Murray, *Nature*, 2006, **439**, 55.

11 S. Srivastava, A. Santos, K. Critchley, K. S. Kim, P. Podsiadlo, K. Sun, J. Lee, C. Xu, G. D. Lilly, S. C. Glotzer and N. A. Kotov, *Science*, 2010, **327**, 1355.

12 B. Kowalczyk, K. J. M. Bishop, I. Lagzi, D. Wang, Y. Wei, S. Han and B. A. Grzybowski, *Nat. Mater.*, 2012, **11**, 227.

13 S. M. Rupich, E. V. Shevchenko, M. I. Bodnarchuk, B. Lee and D. V. Talapin, *J. Am. Chem. Soc.*, 2009, **132**, 289.

14 K. J. M. Bishop, C. E. Wilmer, S. Soh and B. A. Grzybowski, *Small*, 2009, **5**, 1600.

15 D. A. Walker, B. Kowalczyk, M. O. de la Cruz and B. A. Grzybowski, *Nanoscale*, 2011, **3**, 1316.

16 P. Podsiadlo, G. Krylova, B. Lee, K. Critchley, D. J. Gosztola, D. V. Talapin, P. D. Ashby and E. V. Shevchenko, *J. Am. Chem. Soc.*, 2010, **132**, 8953.

17 M. I. Bodnarchuk, M. V. Kovalenko, W. Heiss and D. V. Talapin, *J. Am. Chem. Soc.*, 2010, **132**, 11967.

18 D. V. Talapin, E. V. Shevchenko, A. Kornowski, N. Gaponik, M. Haase, A. L. Rogach and H. Weller, *Adv. Mater.*, 2001, **13**, 1868.

19 P. Simon, E. Rosseeva, I. A. Baburin, L. Liebscher, S. G. Hickey, R. Cardoso-Gil, A. Eychmüller, R. Kniep and W. Carrillo-Cabrera, *Angew. Chem., Int. Ed.*, 2012, **51**, 10776.

20 N. Goubet, H. Portalas, C. Yan, I. Arfaoui, P. A. Albouy, A. Mermet and M. P. Pileni, *J. Am. Chem. Soc.*, 2012, **134**, 3714.

21 R. J. Macfarlane, M. R. Jones, B. Lee, E. Auyeung and C. A. Mirkin, *Science*, 2013, **241**, 1222.

22 Y. Kim, R. J. Macfarlane and C. A. Mirkin, *J. Am. Chem. Soc.*, 2013, **135**, 10342.

23 C. Zhang, R. J. Macfarlane, K. L. Young, H. J. Choi, L. Hao, E. Auyeung, G. Liu, X. Zhou and C. A. Mirkin, *Nat. Mater.*, 2013, **12**, 741.

24 R. J. Macfarlane, M. R. Jones, A. J. Senesi, K. L. Young, B. Lee, J. Wu and C. A. Mirkin, *Angew. Chem., Int. Ed.*, 2010, **49**, 4589.

25 N. R. Jana and X. Peng, *J. Am. Chem. Soc.*, 2003, **125**, 14280–14281.

26 (*a*) P. P. Pillai, S. Huda, B. Kowalczyk and B. A. Grzybowski, *J. Am. Chem. Soc.*, 2013, **135**, 6392; (*b*) D. Witt, R. Klajn, P. Barski and B. A. Grzybowski, *Curr. Org. Chem.*, 2004, **8**, 1763.

27 (*a*) D. W. Wang, R. J. Nap, I. Lagzi, B. Kowalczyk, S. B. Han, B. A. Grzybowski and I. Szleifer, *J. Am. Chem. Soc.*, 2011, **133**, 2192; (*b*) D. W. Wang, B. Kowalczyk, I. Lagzi and B. A. Grzybowski, *J. Phys. Chem. Lett.*, 2010, **1**, 1459.